Burning Rates from Small-Scale Test Motors

Conference Paper · September 2003

CITATION
1

READS
450

5 authors, including:

Luigi T. DeLuca
Politecnico di Milano
399 PUBLICATIONS **2,695** CITATIONS
SEE PROFILE

Filippo Maggi
Politecnico di Milano
140 PUBLICATIONS **941** CITATIONS
SEE PROFILE

R.O. Hessler
23 PUBLICATIONS **33** CITATIONS
SEE PROFILE

BURNING RATES FROM SMALL-SCALE TEST MOTORS

L.T. DeLuca, F. Maggi
Solid Propulsion Lab, Dipartimento di Energetica, Politecnico di Milano
34 Via La Masa, 20158 Milan, Mi, Italy

A. Annovazzi
FiatAvio - Comprensorio BPD, Colleferro, Rm, Italy

R.O. Hessler, R.L. Glick
Somerville, AL, USA and Rensselaer, IN, USA

ABSTRACT

Small-scale solid rocket tests are routinely carried out by propulsion industries to measure burning rate for a variety of needs. Several automated procedures, based on the thickness-over-time and mass balance definitions, are analyzed; particular attention is dedicated to procedures used in Italy and France for quality control of the Ariane-5 launcher solid propellant boosters. Since the actual full-scale burning rates are unknown, results can be compared based only on the statistical quality of the deduced ballistic data. Reproducibility, ease of application, and suitability for automated computer implementation are mainly of interest to industrial users. In this paper, experimental pressure traces from a wide range of small-scale fire tests of Ariane-5 solid boosters are examined. Specific features and general trends of the tested procedures are pointed out. The effects of mix variability, input data quality, and data reduction methods on result reproducibility are discussed. An industrial approach (BSCF) is discussed able to deduce burning surface evolution from pressure traces. Finally, a quasi-steady ballistic technique is proposed and some typical results are reported.

NOMENCLATURE

Latin Symbols

A_b	= burning surface, mm^2
A_t	= throat area, mm^2
a	= coefficient Vieille law, $(mm/s)/(MPa)^n$
c*	= characteristic velocity, mm/s
k	= specific heat ratio
k_{rb}	= burning rate correction factor
M	= mass, kg
n	= pressure exponent Vieille law
p	= pressure, MPa
p_b	= time-averaged pressure, MPa
p_{nb}	= rate-averaged pressure, MPa
r	= rate, mm/s
r_b	= burning rate, mm/s
r_i	= burning rate residual, mm/s
t	= time, s
t_a	= total or action time, s
t_b	= burning time, s
t_{Ei}	= initial burnout time HG method, s
t_{Ef}	= final burnout time HG method, s
T_c	= adiabatic flame temperature, K
V	= volume, mm^3
W	= thickness of propellant web, mm

Greek and other symbols

$\Gamma(k)$	= Vandenkerckhove function
ρ	= density, g/mm^3
σ	= standard deviation
$\Re$	= universal gas constant, J/mole K

Subscripts and Superscripts

A	= beginning of motor operation
avg	= average
b	= burning or burned
B	= beginning of propellant burning
c	= combustion
E	= end of propellant burning
f	= final value
g	= gas
G	= end of motor operation
i	= initial value
max	= maximum value
meas	= measured
p	= propellant
ref	= reference

Abbreviations

BC	= Bayern Chemie
BSCF	= Burning Surface Correction Factor
CV	= Coefficient of Variation
HG	= Hessler and Glick method
IR	= pressure Integral Ratio
MB	= Mass Balance
PM	= Politecnico di Milano
PW	= Pratt & Whitney
S1, S2, S3	= Segment 1, Segment 2, Segment 3
TOT	= Thickness Over Time
WG	= Working Group

1. BACKGROUND

Solid rocket propulsion remains the major propulsion concept for tactical and strategic missiles, and for many first stage launch systems. Knowing burning rate and its dependence from pressure is very important both for rocket design and new propellant formulation. Investigating burning rate under steady or unsteady conditions is also a fundamental step in studies related to applications (performance, costs, ageing of motors) and understanding of burning fundamentals.

The desired values are usually measured in a proper experimental set-up, also because no theory capable to predict burning rates with accuracies within 1% while including the effects of rate modifiers is yet available. In general, subscale test motors are used to determine burning rate during the propellant life cycle (i.e. during research, the initial selection phase for a certain application, in the development and qualification phase of a rocket motor, as batch control during production and ageing studies to determine useful motor life). While providing better correlation with full-scale motor burning rates, small-scale motors are in turn considerably more time- and money-consuming than strand burners. Thus, small-scale motor tests are normally performed after the neighborhood of the final propellant formulation is reached by strand burners, in order to predict full-scale motor rate more accurately. The standard approach is to fire a number of rockets charged with the tested propellant and equipped with pressure transducers.

Ariane-5 solid boosters contain a charge of about 237 t of propellant each. Small-scale test motors used in the booster productive cycle have a cartridge of about 6 kg of propellant. The ultimate goal would be to deduce the booster burning rate pressure dependence, under in-flight conditions, by some data reduction methods. However, because the in-flight acceleration environment is appreciably different from the static firing environment, and because acceleration affects the internal flow and therefore the propellant distortion and the rate, to actually predict flight performance directly from small-motor static firings is questionable. NATO Research and Technology Organization (RTO), Applied Vehicle Technology (AVT), established the Working Group WG-016 (formerly AGARD/PEP WG-27) to assess this kind of methods as used within the international propulsion community. Both simulated and real pressure traces were tested[1] and the outcomes presented at meetings[2-3]. Comparative analyses of more limited scope were previously reported in a series of MSc. Theses[4-5-6-7-8-9] conducted at Politecnico di Milano and other papers[10-11-12-13-14-15-16]. This paper is a follow-up of the WG activities supported by the Italian Space Agency (ASI). Real pressure traces only are analyzed by a variety of methods and using input data from a much wider experimental databank (wholly connected with the Ariane-5 solid boosters). The objectives of the paper are to critically compare these methods, point out the best one (if any), and possibly explore new directions. In this respect, a quasi-steady ballistic technique is proposed and some typical results are reported. Six pressure series from different experimental setups have been tested.

2. DATA REDUCTION METHODS

Based on starting definitions, current approaches to deduce burning rates from pressure traces can be grouped as *Thickness-Over-Time* (TOT) and *Mass Balance* (MB) methods, each including a variety of versions. Real world effects hinder accurate results for either.

2.1 Thickness/Time (TOT) Rate

Burning rate is evaluated, directly, based on the fundamental definition

$$r_{TOT} = \frac{web\ thickness}{burning\ time} = \frac{W_E - W_B}{t_E - t_B} = \frac{W_b}{t_b} \tag{1}$$

requiring the proper value of the burned web thickness, W_b, and the corresponding elapsed burning time $t_b = t_E - t_B$. In actual experiments, W_b and t_b are elusive values. The above definition perform correctly only if burnout is instantaneous. Cylindrically perforated grains are commonly used with the intent to provide a known and uniform web thickness implying also instantaneous burnout. In reality, mandrel misalignment during small-scale motor production, cure and thermal shrinkage produce a grain distortion and the burning front does not reach case walls at the same time in all places causing non-instantaneous burnout. Among the TOT methods, only HG approach accounts for this effect by considering both initial t_{Ei} and final t_{Ef} burnout times. In procedures assuming instantaneous burnout, usually $t_E \cong t_{Ei}$ is set which implies shorter combustion times and higher burning rates.

No standard definitions for the beginning, t_B, and ending, t_E, of burning time exist. Every facility implements its own set of time point definitions[1,17]. Most definitions are either based on some fixed percentage of some characteristic pressure (a maximum or average pressure), or on some attempt to define the "web burnout" or "knee" at the end of the level portion of motor operation. These definitions are essentially arbitrary. HG enforces a set of derivative-based time point definitions[18-19-20].

2.2 Mass Balance (MB) Rate

An alternative approach[21-22-23] based on some approximation of the mass balance equation was in use already around 1960. Burning rate is evaluated, indirectly, from the mass balance between input from the burning propellant grain and output through the nozzle throat. Zero-dimensional transient mass balance with ideal nozzle behavior requires[24]

$$\frac{dp_c}{dt} = \frac{\Gamma^2 c^{*2}}{V_c}(\rho_p - \rho_c)A_b r_b - \frac{\Gamma^2 c^*}{V_c} A_t p_c \tag{2}$$

For $\rho_p >> \rho_c$, quasi-steady burning rate is

$$r_b = \frac{p_c A_t}{c^* \rho_p A_b} \tag{3}$$

Neglecting gas storage in the combustion chamber due to density and/or volume change, an (average) MB rate over the total time of motor operation ($t_a = t_G - t_A$) may be written as

$$r_{MB} = \frac{W_A - W_G}{t_E - t_B}\frac{\int_B^E p_c dt}{\int_A^G p_c dt} = \frac{W_{avg}}{t_b}\frac{\int_B^E p_c dt}{\int_A^G p_c dt} \tag{4}$$

Rate r_{MB} of Eq. 4 differs from rate r_{TOT} of Eq. 1 by a correction factor and compensates[18-19] for the inconsistency between W_A-W_G and W_{avg} by letting $t_E \cong t_{Ei}$. Several variations of Eq. 4 have been used, primarily corrections for the neglect of mass storage, which causes the main error (bias low) in use of the r_{MB} definition. Burning is assumed to occur throughout motor operation, implicitly accounting for non-instantaneous burnout. The average burning surface during burning time is assumed the same as during total time. Although not correct, this assumption approximately accounts for early burnout because of misalignment or distortion, and explains the reduced data scattering reported for MB as compared to TOT methods[25].

2.3 Average Burning Pressures

Two different average pressures, time- and rate-averaged, are in use respectively defined as

$$p_b = \frac{\int_{t_B}^{t_E} p dt}{t_E - t_B} \tag{5}$$

and

$$p_{nb} = \left(\frac{\int_{t_B}^{t_E} p^n dt}{t_E - t_B}\right)^{\frac{1}{n}} \tag{6}$$

Any measured point r_{meas}, $p(r_{meas})$ must simultaneously satisfy also the Vieille burning rate steady law $r = ap^n$, thus use of rate-averaged pressure $p(r_{meas}) \equiv p_{nb}$ is recommended[26-27]. For exponent n less than unity, time-averaged pressure is larger than rate-averaged pressure yielding lower rates corrected to reference pressure. Both the rate correction to reference pressure and the rate-averaged pressure of Eq. 6 require a value of exponent n. This is usually accomplished by performing a least-squares fit of data from multiple motors at different pressures to the Vieille rate equation

$$\ln r_{meas} = \ln a + n \ln p(r_{meas}) \tag{7}$$

For procedures using time-averaged pressure, the least-squares fit of Eq. 7 is performed one time. For procedures using rate-averaged pressure, Eqs. 6 and 7 have to be solved simultaneously by iteration. An iteration beginning with the time-averaged pressure as the starting point (i.e., an initial guess of n = 1) typically converges in three to five steps.

2.4 HG Two-Point TOT Rate

While r_{TOT} will be in error when burnout is non-instantaneous, r_{MB} will always be in error due to neglect of mass storage. HG avoids both errors by a modified r_{TOT} procedure explicitly recognizing non-instantaneous burnout. Two r_{TOT} measurements are made using the average W_{avg} web thickness: r_{bi} using the initial burnout time definition $\boldsymbol{t_{Ei}}$, and r_{bf} using the final burnout time definition $\boldsymbol{t_{Ef}}$. The choices are based on derivative conditions. The final result is

$$r_{HG}\left(p_{nbi}\right) = \frac{1}{2}\left[r_{TOTi} + r_{TOTf}\left(\frac{p_{nbi}}{p_{nbf}} \right)^{n} \right] \tag{8}$$

This procedure, if applied manually, was shown[1,25] to perform very accurately for ideal traces and satisfactorily for real traces. An automated version has also been developed and applied to real traces, but so far it performed not effectively due to excessive pressure measurement noise.

2.5 Classification of Current Data Reduction Methods

Virtually all the burning rate measurements depend on one of the two burning rate definitions above, r_{TOT} and r_{MB}, with various time point definitions. Well-established industrial procedures can be found for both rate definitions. Without a careful experimental validation it is impossible to point out which specific method is actually the best; only relative comparisons can be performed. Based on the implemented kind of average pressure, the two families of current data reduction methods may further be classified as:

Thickness/Time (TOT) Methods

- Time-averaged pressure TOT rate, r_{TOT}
- Rate-averaged pressure TOT rate, r_{TOTn}
- Two-Point rate-averaged pressure TOT rate, r_{HG}

Mass Balance (MB) Methods

- Time-averaged pressure MB rate, r_{MB}
- Rate-averaged pressure MB rate, r_{MBn}

Rate-averaged pressure procedures require an iteration to determine exponent n. TOT procedures, except HG, do not explicitly account for non-instantaneous burnout. Typically, TOT procedures define end of burning as the knee of the curve (web burnout), when the experimental pressure trace begins to fall rapidly near the end of motor operation. However, specific choices of time points may make the correction implicitly. Procedures that define end of burning near 50% pressure implicitly assume burning continuation and thus avoid (at least partly) non-instantaneous burnout error. Due to transient operations, these TOT procedures tend to behave essentially as MB procedures. While use of 50% pressure time points for start of burning only has small effect on burning rate, the choice of 50% or more on fall characterizes a method better than its starting definition.

MB methods yield rates that are systematically low by a mass storage error. In turn, mass storage error introduces a systematic nonlinearity in measured $r_b(p)$. Procedures essentially behaving as MB are likewise low by a mass storage error and generate similar nonlinearities. TOT methods with instantaneous burnout also avoid the mass storage error, yielding negligible nonlinear errors but high bias due to the non-instantaneous burnout commonly occurring in motors.

2.6 Data Reduction Methods Tested in This Paper

The following ten methods, six TOT (of which four used by European industry) and four MB, were tested:

TOT Methods

- BC (Bayern-Chemie, Germany)
- BPD-1 (FiatAvio, Italy)
- BPD-2 (FiatAvio, Italy)
- SNPE (SNPE and ONERA, France)
- HG (Hessler and Glick, USA)

MB Methods

- PM (Politecnico di Milano, Italy)
- PM-n (Politecnico di Milano, Italy)
- PW (Pratt & Whitney, ex-CSD, USA)

BC is a simple but effective time-averaged pressure TOT method used in Germany. BPD-1 is the standard method used by FiatAvio in Italy, while BPD-2 is a modified version[28]; SNPE is used in France with

minor differences by SNPE (absolute pressures) and ONERA (relative pressures). BPD-1, BPD-2, and SNPE are time-averaged pressure TOT methods, iterated to define the time points t_B and t_E but not to determine the exponent n. PM and PM-n are generic MB methods implemented at Politecnico di Milano, using either time- (PM) or rate-averaged (PM-n) pressure. PW is a time-averaged pressure MB method used by Pratt & Whitney (formerly CSD) in USA; PW has been implemented with t_B=10% p_{max} and t_E corresponding to a range of values associated with a more or less large fraction (Integral Ratio, IR) of the total pressure integral (by choosing different IR's). HG is a two-point, rate-averaged pressure, TOT method.

In all cases tested in this paper, absolute pressures were used; burning rates were deduced from the nominal web thickness; and the total or action time t_a of MB methods was computed as the time span during which pressure is over a threshold value of 1% of the pressure transducer full-scale range. All methods, except those developed at Politecnico di Milano, are fully described in the WG-016 report[1].

Independent on their conceptual origin, all methods - except HG - are similar in their final implementation and may even overlap stemming from the poor handling of transient burning, especially TOT tail off. For example, BC is originally derived as a TOT method by defining a time span during which pressure is over a threshold value of 0.2 MPa, but enforces a 50% burning time definition compensating to some extent for non-instantaneous burnout (although not as well as a MB method).

3. ARIANE-5 SOLID BOOSTERS EXPERIMENTAL DATA

Experimental pressure traces were collected from several series of Baria small-scale tests performed for batch and quality control of the S1 segment of Ariane-5 boosters; but for a matter of space only three series (S1-013, S1-027, S1-A2) are here reported. Likewise, four series of tests were conducted for segments S2 and S3 having a slightly larger burning rate; but for a matter of space only three series (S2-A2, S3-A2, and S3-031) are here reported. Baria test motor is used in France and, with modifications, in Italy. Each test series consisted of 9 (S1 segment) or 10 replicate mixes (S2 and S3 segments) of the same propellant; for each mix 3 motors were tested at different pressures (nominally: 3, 4.5, 7 MPa) for a total of 27 or 30 fire tests per series. The reference pressure is 4.5 MPa (45 bar). All runs were conducted either by FiatAvio – Comprensorio BPD (located at Colleferro, near Rome, Italy) or by Regulus in the Ariane-5 production plant (located in Kourou, French Guyana).

A systematic comparison of European industrial TOT methods was specifically conducted. BPD-1, BPD-2, and SNPE techniques were run in[7-8-9] but also checked with the actual method originators in Italy[28] and France[29] usually with minor differences. All procedures were tested automatically.

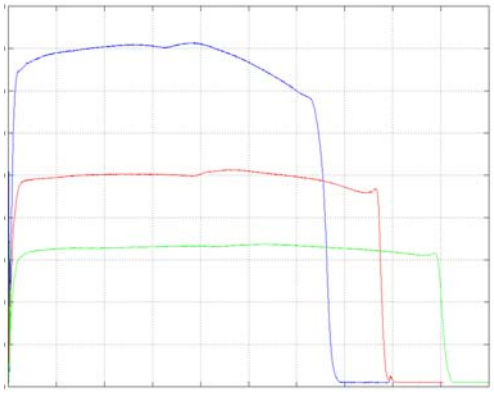

Fig. 1a. Experimental pressure traces vs. time for a propellant mix (S1 by FiatAvio).

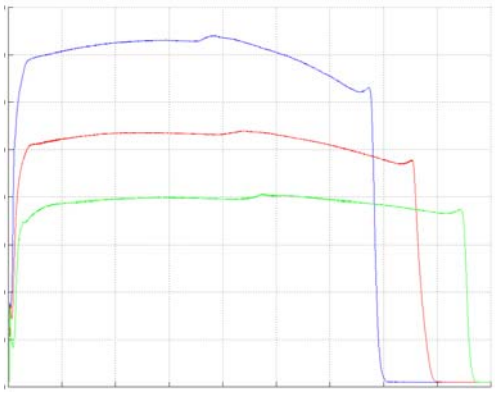

Fig. 1b. Experimental pressure traces vs. time for a propellant mix (S2, S3 by Regulus).

3.1 Experimental Pressure Traces

For each mix of each S1 (FiatAvio), S2 (Regulus), and S3 (Regulus) series, a group of three experimental pressure traces is obtained from Baria testing. In Figs. 1a-1b pressure traces from different experimental setups and manufacturers are reported. Although similar, single pressure traces may be different in details. In particular, pressure traces do not overlap during ignition making difficult to detect the pressure history beginning. The Baria propellant grain is designed to obtain an almost constant pressure. Inspection of Figs. 1a-1b shows that while low pressure level roughly fulfils the requirement, the behavior worsens with the increase of pressure.

3.2 Survey of Baria Results

Although mixes are intended to be identical and burn with identical rates, small differences in the propellant manufacture, test motor manufacture, instrumentation, test operations, or data analyses cause the measured burning rates to scatter. Analysis of these differences can be used to estimate the contributions of the various sources of the scatter. It is convenient to distinguish the "test variability" (induced by propellant mix or batch, motor hardware, instrumentation, and testing operations) from the "procedure variability" induced by the data reduction technique. Results clearly show that for each data reduction method, ballistic parameters do depend on test. Likewise, for each test, ballistic parameters depend on the implemented method but featuring some consistent trends (to be discussed). Thus, the unavoidable test data variability due to a variety of practical reasons is intermingled in unknown ways with the selected procedure variability. This interaction occurs for all variability sources (propellant, motor, instrumentation, and testing operations) and is further confused by the statistical fluctuations of composite propellant formulation[30].

The burning rate data from each mix were reduced separately for each procedure and least-squares fitted to the Vieille steady rate equation $r_b = ap^n$. Then, for each series the average values of the ballistic parameters (a and n) parameters describing the different batches were obtained. For each series, ballistic results (mean values ± standard deviation σ and coefficients of variation CV=100•σ /mean value) are reported at the reference pressure of 4.5 MPa (45 bar) in Tables 1a-1b (S1 tests by FiatAvio), Table 1d (S2 tests by Regulus), and Tables 1f (S3 tests by Regulus).

3.3 General Remarks on Tested Data Reduction Methods

Examination of Tables 1a-1f provides an assessment at the same time about test variability for each given procedure and about procedure variability for each data series. Overall, the above tables indicate that the European industrial TOT methods nominally assuming instantaneous burnout (BC, BPD-1, BPD-2, SNPE) produce mean values that are quite similar, as expected from the general similarity of these procedures. Within this group, BPD-2 and SNPE (which differ only in details) produce about the same results, while BC yields reasonable results with a particularly simple computational scheme. Thiokol methods seem to require further refinements in the current implementation. The flexible PW method selects the burning time by defining a fraction of the total pressure integral by means of the tunable parameter IR, to be adapted - based on experience - to each specific motor configuration. In Table 1a, old (POLIMI) and new (PM) implementations of the generic MB methods by Politecnico di Milano are also compared, with t_B=10% p_{max} for all versions. The new versions (PM and PM-n) implement a standard bisector procedure to define the burnout instant and thus behave properly even when the Friedman's curl, usually occurring before final pressure fall down, is not clearly detectable in the pressure traces. In Table 1a, an application of the manual HG method is also reported.

MB methods yield rates that are systematically low by a mass storage error. In turn, mass storage error introduces a systematic nonlinearity in measured $r_b(p)$. Procedures essentially behaving as MB are likewise low by a mass storage error and generate similar nonlinearities. TOT methods with instantaneous burnout also avoid the mass storage error, yielding negligible nonlinear errors but high bias due to non-instantaneous burnout.

Table 1. Ballistic parameters (mean ± σ and CV values) at 4.5 MPa reference pressure

a. Baria series S1-013 (9 groups of fire tests)

	$n \pm \sigma_n$	CVn, %	$a \pm \sigma_a$	CVa, %	$r_b \pm \sigma_{rb}$	CVr_b, %
BC	0.3817 ± 0.0044	1.166	4.1659 ± 0.0268	0.642	7.3961 ± 0.0229	0.309
BPD-1	0.3826 ± 0.0048	1.255	4.1624 ± 0.0285	0.683	7.4001 ± 0.0225	0.304
BPD-2	0.3805 ± 0.0043	1.138	4.1647 ± 0.0270	0.648	7.3807 ± 0.0233	0.316
SNPE	0.3808 ± 0.0035	0.929	4.1624 ± 0.0216	0.518	7.3801 ± 0.0241	0.327
HG	0.3787 ± 0.0039	1.022	4.2082 ± 0.0182	0.433	7.4376 ± 0.0198	0.266
POLIMI	0.3755 ± 0.0035	0.924	4.1828 ± 0.0219	0.524	7.3573 ± 0.0234	0.319
PM	0.3753 ± 0.0035	0.926	4.1835 ± 0.0220	0.526	7.3562 ± 0.0238	0.324
POLIMI-n	0.3763 ± 0.0036	0.954	4.1809 ± 0.0219	0.525	7.3635 ± 0.0232	0.316
PM-n	0.3761 ± 0.0036	0.956	4.1815 ± 0.0220	0.526	7.3623 ± 0.0236	0.321
PW (IR=.985)	0.3762 ± 0.0059	1.562	4.2362 ± 0.0469	1.106	7.4591 ± 0.0326	0.437
PW (IR=.995)	0.3795 ± 0.0068	1.800	4.1696 ± 0.0516	1.238	7.3786 ± 0.0324	0.439

b. Baria series S1-027 (9 groups of fire tests)

	$n \pm \sigma_n$	CVn, %	$a \pm \sigma_a$	CVa, %	$r_b \pm \sigma_{rb}$	CVr_b, %
BC	0.3933 ± 0.0046	1.1681	4.1054 ± 0.0293	0.7133	7.4179 ± 0.0329	0.4436
BPD-1	0.3939 ± 0.0048	1.2136	4.1038 ± 0.0307	0.7488	7.4217 ± 0.0336	0.4521
BPD-2	0.3921 ± 0.0046	1.1786	4.1039 ± 0.0299	0.7275	7.4016 ± 0.0330	0.4453
SNPE	0.3942 ± 0.0046	1.1589	4.0858 ± 0.0314	0.7682	7.3916 ± 0.0342	0.4630
PM	0.3871 ± 0.0043	1.1160	4.1193 ± 0.0294	0.7130	7.3732 ± 0.0336	0.4557
PM-n	0.3880 ± 0.0044	1.1362	4.1171 ± 0.0291	0.7062	7.3797 ± 0.0336	0.4550
PW (IR=.985)	0.3866 ± 0.0045	1.1546	4.1846 ± 0.0306	0.7319	7.4851 ± 0.0340	0.4538
PW (IR=.995)	0.3882 ± 0.0041	1.0677	4.1281 ± 0.0255	0.6167	7.4019 ± 0.0320	0.4322

c. Baria series S2-A2 (10 groups of fire tests)

	$n \pm \sigma_n$	CVn, %	$a \pm \sigma_a$	CVa, %	$r_b \pm \sigma_{rb}$	CVr_b, %
BC	0.3901 ± 0.0087	2.233	4.1752 ± 0.0587	1.406	7.5145 ± 0.0199	0.2643
BPD-1	0.3900 ± 0.0090	2.231	4.1835 ± 0.0624	1.492	7.5201 ± 0.0212	0.2813
BPD-2	0.3911 ± 0.0080	2.050	4.1609 ± 0.0526	1.263	7.4930 ± 0.0182	0.2424
SNPE	0.3911 ± 0.0080	2.034	4.0619 ± 0.0523	1.256	7.4941 ± 0.0183	0.2444
PM	0.3942 ± 0.0073	1.846	4.1073 ± 0.0448	1.091	7.4306 ± 0.0162	0.2174
PM-n	0.3942 ± 0.0072	1.819	4.1147 ± 0.0437	1.061	7.4444 ± 0.0158	0.2126
PW (IR=.985)	0.3930 ± 0.0073	1.868	4.1798 ± 0.0488	1.168	7.5480 ± 0.0191	0.2525
PW (IR=.995)	0.3923 ± 0.0078	1.976	4.1372 ± 0.0518	1.253	7.4636 ± 0.0191	0.2565

d. Baria series S3-031 (10 groups of fire tests)

	$n \pm \sigma_n$	CVn, %	$a \pm \sigma_a$	CVa, %	$r_b \pm \sigma_{rb}$	CVr_b, %
BC	0.3768±0.0049	1.307	4.2969±0.0417	0.971	7.5681±0.0262	0.346
BPD1	0.3768±0.0052	1.383	4.2957±0.0440	1.025	7.5706±0.0267	0.353
BPD2	0.3766±0.0042	1.110	4.2847±0.0353	0.824	7.5497±0.0245	0.324
SNPE	0.3764±0.0045	1.189	4.2871±0.0379	0.884	7.5511±0.0251	0.332
PM	0.3775±0.0039	1.024	4.2471±0.0283	0.667	7.4930±0.0216	0.288
PMn	0.3778±0.0034	0.894	4.2513±0.0252	0.592	7.5045±0.0214	0.285
PW(IR=.985)	0.3775±0.0039	1.026	4.3122±0.0292	0.678	7.6085±0.0223	0.293
PW(IR=.995)	0.3764±0.0039	1.047	4.2719±0.0290	0.679	7.5245±0.0209	0.278

Comparing reduction methods indicates that, relative to the industrial TOT methods, PM and PM-n consistently produce lower rates while HG produce higher rates. Analysis of simulated data also indicates[20] that in general MB procedures, relative to the industrial TOT methods, intrinsically underestimate exponent because of neglected mass storage. This is observed in the real pressure traces measured in S1 experimental setups but not in S2 and S3 setups.

PW results – and in particular burning rates - depend on the value of the IR ratio, in turn depending upon the chamber volume and propellant charge. As such, IR should be defined independently for each motor design and accordingly PW results will depend on its value. Since the standard IR=0.98 suggested for untested motors seemed too low, values from 0.975 up to 1.0 were run in this investigation revealing a nonlinear effect on the deduced ballistic results. For the reported values of IR=0.985 and 0.995, PW rates decrease for increasing IR and are typically larger than PM or PM-n rates.

PM detects t_E at the knee of the curve, for which the non-neutrality error will be less than for the industrial TOT methods, which all define t_E much later, when pressure has declined to around 50%. Time-averaged pressure is greater than rate-averaged pressure, so any procedure using time-averaged pressure yield a rate equation that is consistently biased low due to the non-neutrality error. Thus, PM-n (or POLIMI-n) is expected to yield comparatively higher rates and exponents than PM (or POLIMI). As a matter of fact, the rate-averaged pressure used by PM-n (or POLIMI-n) systematically makes the resulting ballistic law a bit faster, say by 0.1% in S1 and 0.2% in S2 or S3, indicating that the error due to non-neutral burning also depends on the specific Baria experimental setup.

3.4 Assessing Test Variability

To explain more subtle features, one needs to examine the detailed raw results (effective time, effective pressure, and burning rate) obtained for each mix of a given procedure. Some of these were reported[12] for S1 in the bar plots of Fig. 2 (effective burning time), Fig. 3 (effective burning rate), and Fig. 4 (effective burning pressure) at the lowest of the 3 operating pressures, where the best data quality was obtained; however, similar trends are found at other pressures. To avoid confusion, the discussion will concentrate on methods using time-averaged pressure (BC, BPD-1, BPD-2, POLIMI, and SNPE) and will focus on the industrial TOT methods. For the industrial TOT methods using time-averaged pressure (BC, BPD-1, BPD-2, and SNPE), the controlling factors are the (average) effective pressure and effective time (interval) of the combustion process, affecting respectively burning rate and data reproducibility. The effective time and deduced burning rates *(at the relevant effective pressure)* are about the same for all TOT methods. However, as far as effective pressure is concerned, BC and BPD-1 yield close but smaller values than SNPE and BPD-2, in turn very close; this gap increases with operating pressure. The final outcome is that BC and BPD-1 produce larger exponent *n* and burning rates with respect to SNPE and BPD-2. Therefore, it is the way that each method handles pressure through the pressure integral (and thus accounts for ignition and burnout transients, combustion anomalies, noisy traces, etc.) that makes the difference. The PW method uses the IR value to deduce both the effective time, and indirectly the effective pressure. The possibility to tune up the method exists but a massive test campaign is needed to choose the proper IR value for a type of experimental setup. The interaction between effective pressure and time has been analyzed in a M. SC. Thesis[9].

The quality of the obtained data is relatively good for low pressure fire testing, but worsens for medium and high-pressure tests. This trend is observed for all methods, as shown in Fig. 5 reporting the CV values obtained for effective time, effective pressure, and burning rate of the S1-013 series. The effective pressure is by far the most serious offender and its accuracy worsens by a factor of 2 (high pressure) to 3 (medium pressure) with respect to low-pressure findings. Thus, experimental data of better quality (in terms of reduced test variability and improved pressure traces accuracy) are strongly needed.

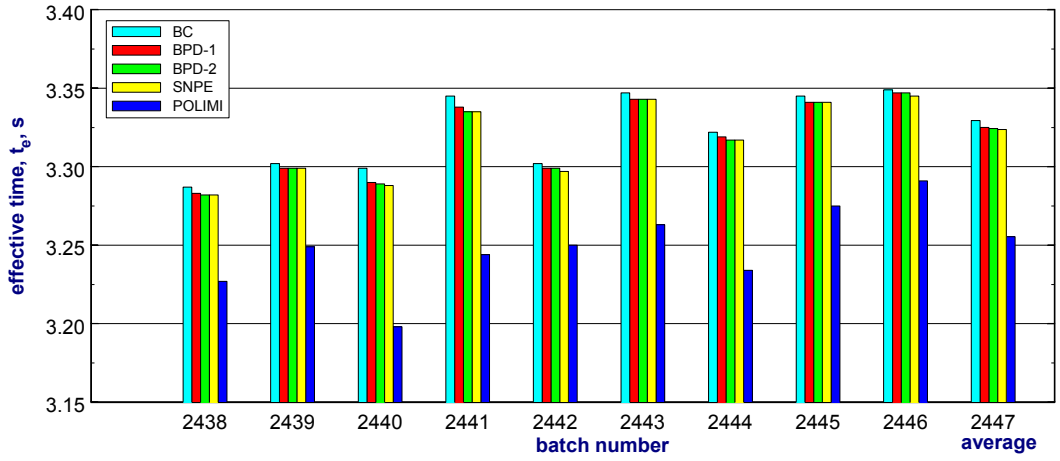

Fig. 2. Effective time of Baria series S1-013 varying with tests but little dependent on implemented TOT methods at low operating pressures (2447 is a dummy batch for average values).

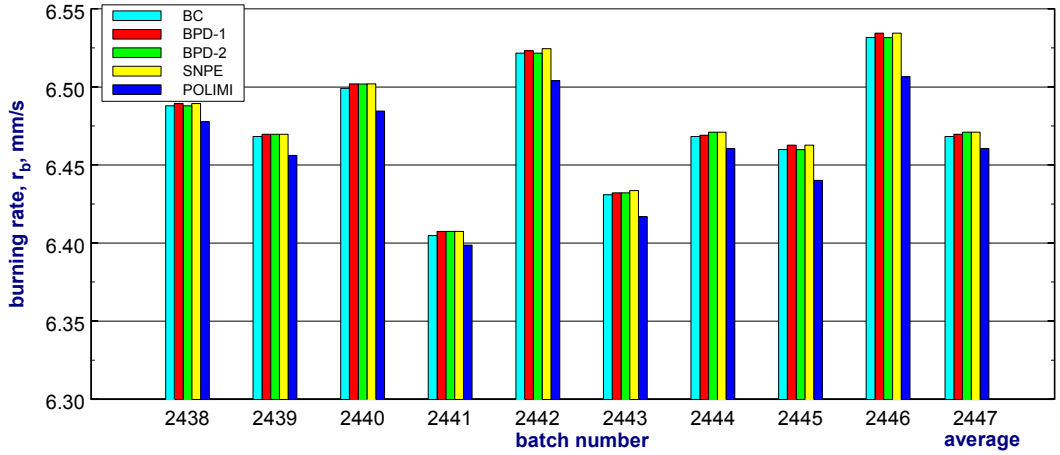

Fig. 3. Burning rate of Baria series S1-013 varying with tests but little dependent on implemented TOT methods at low operating pressures (2447 is a dummy batch reporting average values).

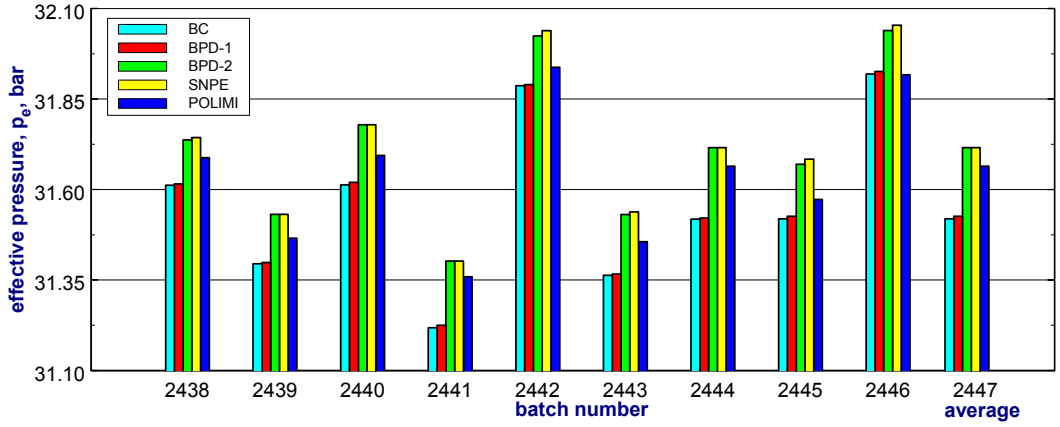

Fig. 4. Effective pressure of Baria series S1-013 varying with tests and also dependent on implemented TOT methods at low operating pressures (2447 is a dummy batch reporting average values).

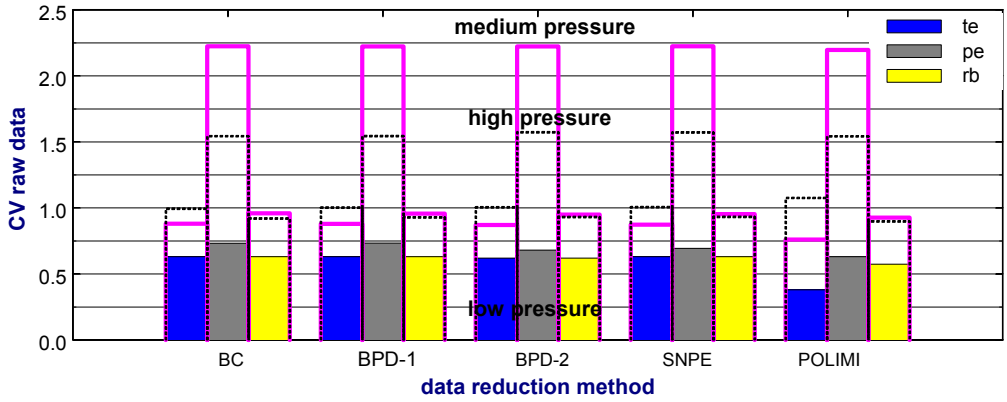

Fig. 5. CV of Baria series S1-013 worsening with increasing test pressure for all reported methods; effective pressure (central bar) at medium (magenta) and high (dashed) test pressures is the worst offender.

3.5 Assessing Series Variability

The CV of the normalized ballistic parameters were investigated for several S1 series. The r_b scatter (see Fig. 6) is remarkably the same for all industrial methods, while the CV results of the manual HG procedure in general do not always align with those from the automated procedures. However, the most striking effect is that results are essentially similar for a given S1 series but change from series to series: for example, r_b scatter of S1-018 is several times (4 to 5) that of S1-016. Scatter of exponent n is about twice that of factor a (not shown for a matter of space); since n is a parameter of intrinsic poor accuracy, its CV contains a sizeable component of all pertinent data variations.

3.6 Assessing Overall Data Quality

Taking another viewpoint, the overall data quality of a given series can be assessed by contrasting the burning rates obtained by each procedure against the reference quasi-steady values of Eq. 3. This is a mass balance requiring accurate knowledge of the average combustion pressure (p_c), effective nozzle throat area ($\eta_t A_t$), propellant density (ρ_p), burning surface (A_b), and characteristic velocity (c^*). The effective nozzle throat area may be determined by measuring the geometrical nozzle throat diameter. The factor η_t may be based on experience, and may be different for each nozzle, propellant and combustion pressure; its choice may be ambiguous and this can produce additional errors. The propellant density may be either measured or calculated. The burning surface area may be calculated based on accurate measured grain dimensions. The burning surface is constant for the case of an end-burning grain (coning is not considered), but will generally change with time when a cylindrically perforated grain is used. Finally, under ideal operations, the characteristic velocity is fully determined by the adiabatic equilibrium properties of the propellant combustion products

$$c_{th}^* = \frac{1}{\Gamma(k)}\sqrt{\frac{\Re}{M}T_c} \tag{9}$$

Assuming for simplicity η_t =1 and inserting the proper values of relevant parameters in Eqs. 3 and 9, the linear plots (for practical reasons) of Fig. 7 were obtained for the medium pressure tests of Baria S1-013 series (reference). It is seen that BC and BPD-1, on one hand, and SNPE and BPD-2 on the other hand essentially overlap. POLIMI-n is shifted horizontally (in pressure) with respect to POLIMI due to the use of rate-averaged rather than time-averaged pressure. SNPE and BPD-2 rates are placed low with respect to the reference line; HG is high at high pressure; PW position depends on IR value (IR=0.985 is biased high, while IR=0.995 goes from low to high for increasing pressure). At low (not shown for a matter of space) and medium (Fig. 7) pressures, BC, BPD-1, and HG data are the closest to the reference line; at high pressure (not shown for a matter of space), POLIMI-n data are the closest.

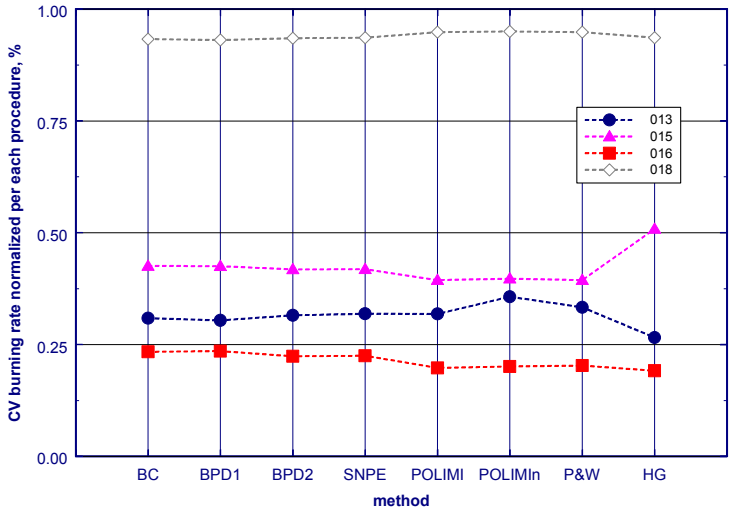

Fig. 6. Baria S1: CV of normalized rate r_b depending on experimental data series.

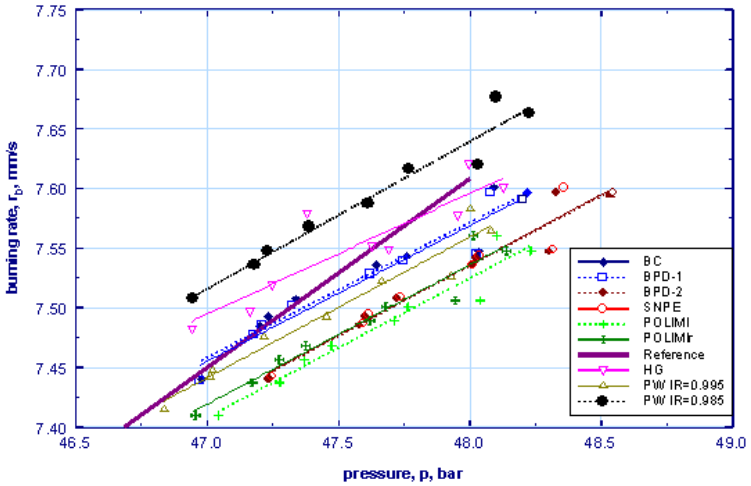

Fig. 7. Baria S1-013: medium pressure burning rate fitting of several procedures.

3.7 Assessing Effects of Data Reduction Methods

Visual inspection of Figs. 2-4 suggests some general trends for BC, BPD-1, BPD-2, SNPE, and PM methods. Due to the different approach implemented (MB vs. TOT), PM systematically brings about a shorter effective time compared to TOT methods and smaller burning rate, while the corresponding effective pressure is intermediate between SNPE / BPD-2 on one hand and BC / BPD-1 on the other hand (but getting closer to BC / BPD-1 at high pressure). PM-n yields the same effective time of PM, but a lower effective pressure and thus larger reference burning rate due to use of the rate–averaged pressure.

In general, for pressure traces featuring short as well as smooth ignition and burnout transients, a relatively long effective time accounting for non-instantaneous burnout should be considered. But for pressure traces featuring protracted and irregular transients, especially during ignition, a short effective time may yield better reproducibility. The influence of different end burning points and thus effective times was carefully checked for PM[8], showing that the good results of this technique (Tables 1) are due to the short effective time selected (about 97-98% of web burned).

3.8 Assessing Test vs. Procedure Variability

An attempt was made to distinguish the influence of test variability on the results from that of the data reduction method. All obtained ballistic data (a, n, r_b) were "self-normalized" to remove the influence of the implemented method. For each procedure, the average ballistic values of a given series were

computed and normalized values = actual value / average value were deduced. For example, the normalized burning rate of a given data series was computed as actual burning rate / average burning rate for each batch of that series; the normalization or average value is different for each procedure and each data series. This self-normalization process was performed for all methods and most data series. Examples of the resulting normalized plots are reported in Fig. 8 (series S1–013) and Figs. 9-11 (series S1–027). Just for check in all figures, besides the 9 test batches, an additional dummy batch corresponding to the normalized average burning rate of each procedure (by definition, 1 in all cases) is reported.

Normalized burning rate trends may sensibly vary from series to series (for example, see Figs. 8-9). Yet it is remarkable that:

- The test-to-test variation within a series is generally very close, say within 0.5%.
- However, appreciably larger differences do intermittently occur between batches within the same data series, even using the same procedure.
- HG method, being subjected to human error because of its manual implementation, appears to result in less reproducible trends compared to automated methods.
- Considering all results (only a few are reported for matter of space), the family of 4 industrial TOT methods and the family of MB methods, as run in this paper, display each virtually identical results; however the two trends, although very similar, are distinct.
- Variations of burning rates among tests, within a given series or from series to series, are markedly larger than variations due to procedures. In other words, the repeatability of the various procedures is better than the burning rate repeatability of the tests.

A more complete understanding can be obtained by inspecting also the normalized values of the ballistic parameters a and n. For example, see Figs. 10-11 for series S1-027. Both a and n are essentially within 2% accuracy. But the two plots feature opposite trends (a increases when n decreases, and vice versa) due to the enforced Vieille law. The trend of n is less regular due to an inherent problem in exponent measurement, because by definition $n = \partial(\ln r_b)/\partial(\ln p)$ is a partial derivative in pressure (keeping constant any other operating conditions). This definition magnifies the effect of "noise" (differences in propellant, motor, instrumentation, or testing operations) and makes n measurement less accurate.
In conclusion, the normalized values of the ballistic parameters illustrated in Figs. 10-11 point out that variability of the various procedures - although may sensibly vary from series to series and features different patterns for a and n - is ultimately much less important that variability of experimental data from at least S1 small-scale test motors. Despite minor differences here and there, overall all automated methods – once normalized to remove the effect of the specific method - show the same variability especially in terms of burning rate.

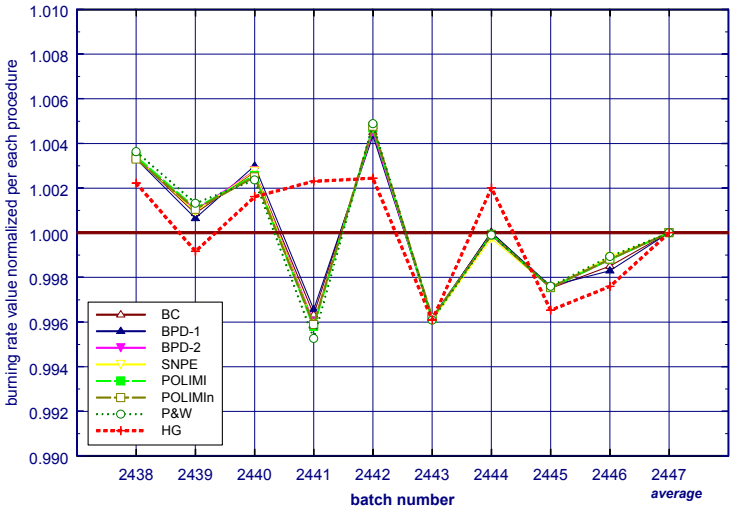

Fig. 8. Baria S1-013: manual HG does not exactly follow the trend of automated procedures for normalized burning rate (at reference pressure).

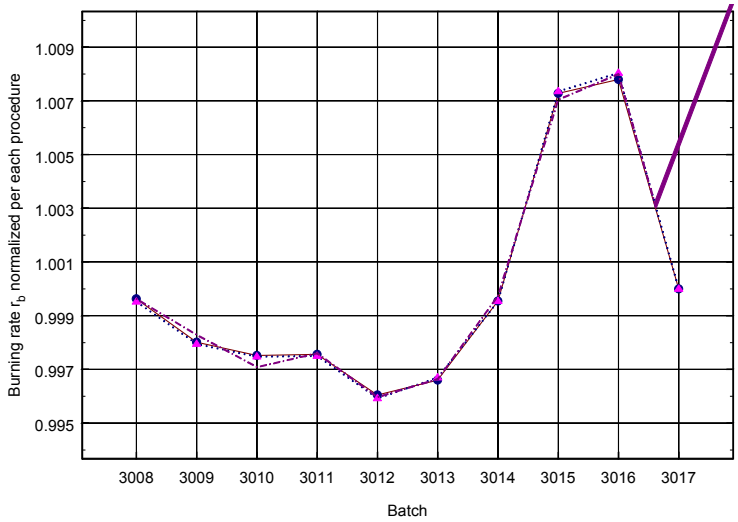

Fig. 9. Baria S1-027: normalized burning rate is essentially the same for all tested methods.

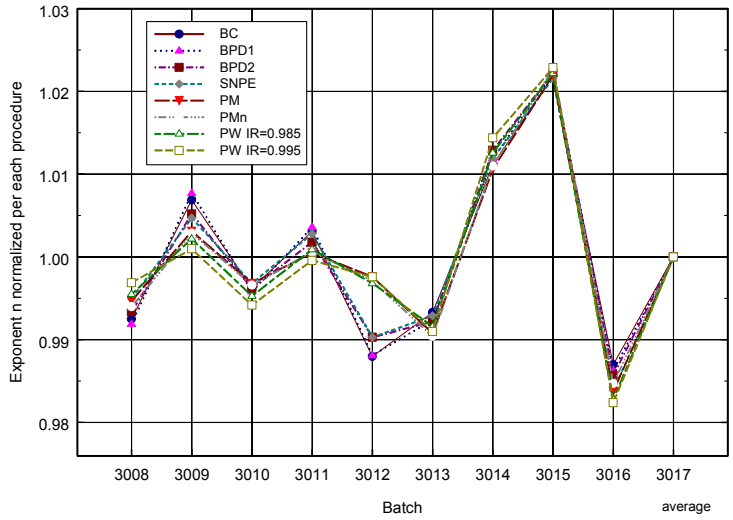

Fig. 10. Baria S1-027: normalized pressure exponent *n* featuring differences for batch 3012.

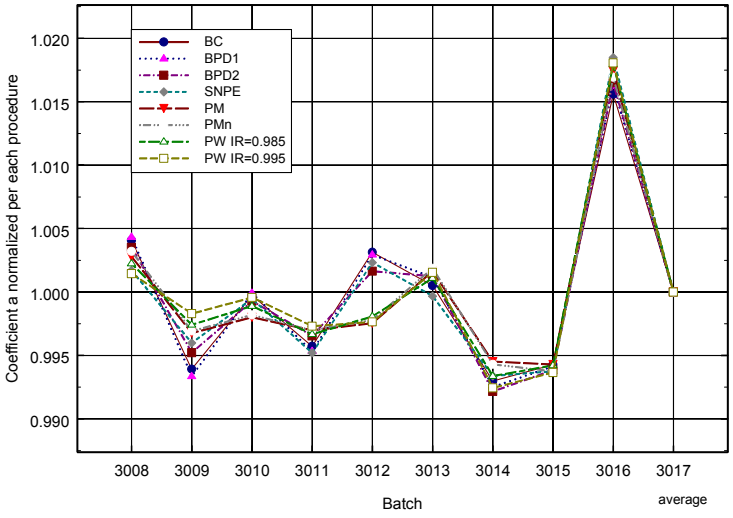

Fig. 11. Baria S1-027: normalized factor *a* featuring differences for batch 3012.

4. BURNING SURFACE CORRECTION FACTOR (BSCF)

Since all data reduction procedures so far discussed only give an average ballistic characterization of the propellant, an approach capable to follow the combustion phenomena history is of interest. A specific procedure used by FiatAvio and other industries, mainly in USA and France, is meant to compare the actual burning surface evolution (i.e., deduced by pressure traces) vs. the theoretical evolution (i.e., based on motor design). The instant-by-instant comparison between these two calculated quantities provides a parameter, called BSCF (Burning Surface Correction Factor), as a function of the propellant web thickness

$$BSCF = \frac{Real\ Burning\ Surface}{Ideal\ Burning\ Surface} \tag{10}$$

As a matter of fact, different propellant grains may feature a different behavior even if they are from the same propellant batch. This can lead results of data reduction methods to be non fully representative of the tested propellant. The BSCF parameter analysis can shed light non reproducibility effects among different tests belonging to a single series. This information cannot be obtained by the commonly implemented data reduction methods because they average the motor performance.

4.1 The BSCF Procedure

Both real and ideal surfaces are needed to perform this analysis. Burning rate is supposed to be uniform along the burning surface for either cases. If the geometrical grain size is known, the ideal burning surface is easily obtained as a function of the propellant web thickness; this function is independent on the burning rate value. On the contrary, the real burning surface is computed through a mass balance equation as shown in what follows.

Under quasi-steady conditions, considering $\rho_p >> \rho_c$ and considering also an ideal nozzle behavior, the governing zero-dimensional mass balance equation is easily derived from Eq. 2. The experimental characteristic velocity c* can be evaluated as

$$c^* = c_{th}^* \quad \eta_{c^*} \tag{11}$$

where the theoretical c^*_{th} value, obtained for a given propellant formulation by a chemical equilibrium computer code, is found slightly pressure dependent (see Eq. 9). In turn, the η_{c^*} efficiency can be calculated as

$$\eta_{c^*} = \frac{1}{M_p}\int_0^{t_b} \dot{m}\, dt = \frac{1}{M_p}\int_0^{t_b} \frac{A_t p_c(t)}{c^*_{th}}\, dt \tag{12}$$

where M_p is the loaded propellant mass and $p_c(t)$ the measured instantaneous chamber pressure.

By taking into account Vieille law, the burnt web definition, and the mass balance equation, the following system can be solved to evaluate burning surface and web in time, and thus $A_b(w)$:

$$\begin{cases} A_b(t) = \dfrac{A_t p_c(t)^{1-n}}{\rho_p a c^*} \\ w(t) = a\displaystyle\int_0^t p_c(t)^n \ dt \end{cases}$$

The ballistic parameters *a* and *n* can be obtained from any of the previously discussed standard industrial procedures.

In Fig. 12 an example of this technique applied to a series of 30 pressure traces (10 per each of the three tested pressure levels) is shown for the S3-031 Baria test. This graphical representation gives a qualitative indication of single tests repeatability of the experimental burning surface due to the typical scattering of the small-scale test motor behavior. For example: non uniform ignition, non homogeneous grain burn rate, shifting of the real grain configuration with respect to the design, and so on. Instead, in the ideal case, this burn surface would be the same for each motor functioning condition (invariant of the ballistic problem). For this ideal reason, the average of the above surface traces is made in order to define an reference burning surface versus web for the S3-031 Baria tests.

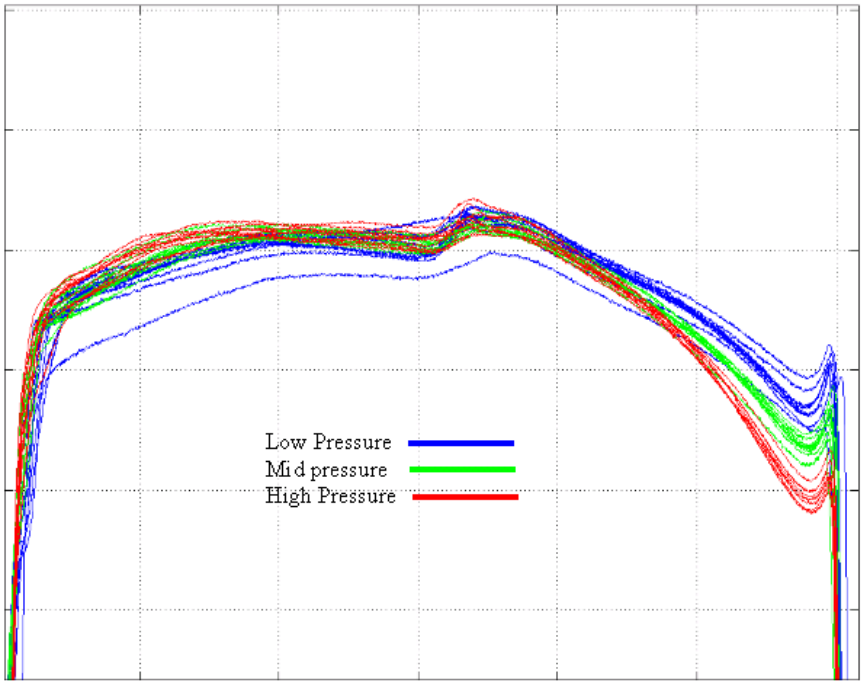

Fig. 12. Baria S3-031: actual burning surface vs. burnt propellant thickness for 10 groups of pressure traces.

The geometrical evolution of the burning surface may differ due to different raw materials, casting, curing, etc. of the propellant grain. Within one test series the behavior after ignition is quite uniform, except for some obviously defective shots, while the end behavior points out higher burning surfaces for decreasing operating pressure. This general trend was observed for several test series, although anomalies might occasionally be evidenced.

Based on the firing test of S3-031 Baria, an average burning surface $A_{b,ave}(w)$ can be obtained as representative of that series (reference); some typical results obtained for series S2-A2 and S3-031 are reported in Fig. 13 (BSCF factor). The BSCF procedure can also be used to deduce a burn rate measurement[9].

4.2 Comments upon Results

The BSCF method has been implemented to show burning surface evolution during combustion. This can help both to understand if test motor behaves as ideally expected and to single out anomalies within a series. For the cast-in-place mandrel test series shown in Figs. 12-13, two effects are evident. Concerning the burning surfaces of single test within a series (Fig. 12), reproducibility of the curves appears good in the first half of the combustion process, bad in the second half where curves separate depending on the pressure level (higher pressures imply lower end-burning surface). Concerning the average burning surface of a whole series (Fig. 13), the *BSCF* coefficient shows that the surface regression is not ideal: burning surface is overestimated in the first half of the combustion process and underestimated in the final part. Both findings confirm that the industrial burning rate reduction methods introduce implicit assumptions that are not verified in reality.

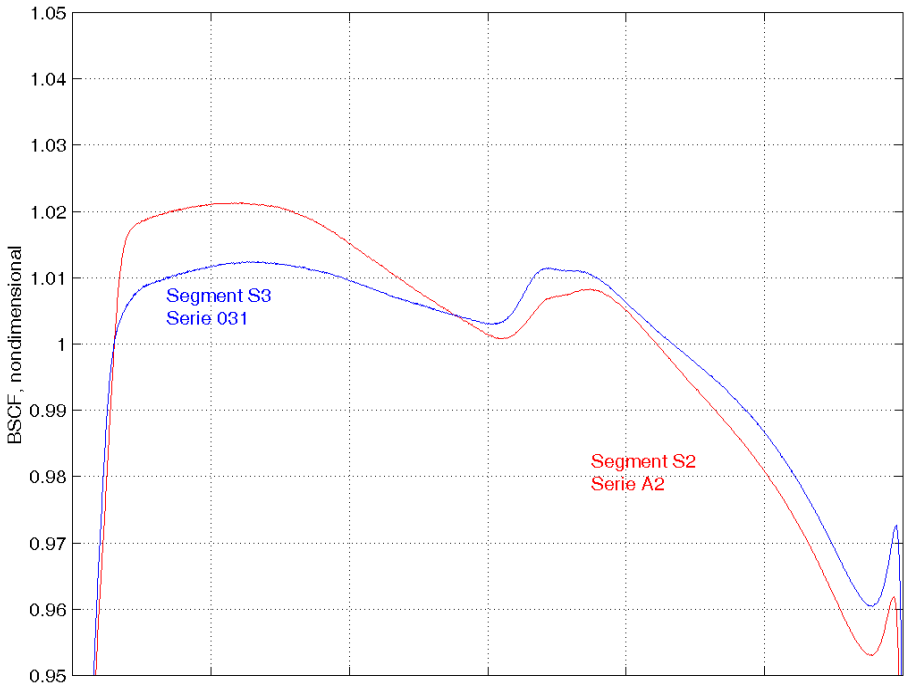

Fig. 13. BSCF parameter evaluated vs. burnt propellant thickness for S3-031 and S2-A2 series.

4.3 Comments upon BSCF Method

Even if the BSCF method is a step forward in the analysis, problems and limitations exist. The method needs as input ballistic parameters taken from a standard industrial procedure; thus, if used to deduce burning rates, the results will be affected by the same possible errors affecting the implemented industrial procedure. The additional information obtained by the BSCF method (such as surface evolution vs. web) adds considerations upon the tested motors useful to assess the test quality and reliability. Moreover, the calculated surface is correct only to the extent that the propellant surface regresses regularly, without any distortion (as implicitly assumed). But it is known that propellant grains are subject to shrinkage and distortion processes due to thermal stress; also, chemical composition gradients due to casting may locally affect burning rates. Finally, all mass balance equations may be affected by the errors already mentioned in Section 2.2.

5. A QUASI-STEADY BALLISTIC METHOD

All of the data reduction methods so far discussed analyze pressure traces from small scale test-motors under the basic assumptions that the grain combustion surface is constant and burning rate uniform. Notwithstanding severe efforts to make this true, in Baria as well as other test motors, a variety of real world effects (including propellant casting and processing[31-32], wall effects, grain geometry, etc.) bring about a nonuniform burning rate overlapping with a non constant burning surface. Therefore, the experimental pressure trace are far from the expected ideal behavior (as shown in Figs. 12-14). For all data reduction methods so far discussed, the final result is some kind of unknown "average" of the burning rate.

A possible approach to overcome these basic difficulties is to account for the instantaneous ballistic behavior of the motor under examination during the quasi-steady portion of the whole burning process. Also because of the industrial environment, the model has to be as simple as possible and competitive with the current techniques in terms of both time and difficulty.

5.1 The Proposed Model

The developed software takes in consideration quasi-stationary equations for the combustion process with a parameter to adjust burning rate during combustion. Transient burning is not modeled and thus the very beginning and end of pressure traces are not expected to be reproduced. Mass storage is neglected during combustion but taken into account after burnout to simulate the motor evacuation through the sonic nozzle. The burning surface of the propellant grain is assumed plain and regular, but of changing size during combustion.

Mass balance is computed as already discussed in Section 2.2, but a more general form of the standard Vieille burning rate law was implemented in an attempt to overlap the computed and experimental pressure traces

$$r_b = a(w)\ p^n$$

For a given initial temperature, the Vieille coefficient is seen as a function of the burned web thickness a = a (w). In general, the a(w) function is deduced "point-by-point" from a fitting procedure repeated at each web thickness. For Baria motors with mandrel-in-place casting, a parabolic function is obtained for a(w). This result underlies the well-known[33] anisotropic ballistic behavior of cast composite propellants, by which burning rates are affected by solid particle orientation established during casting of cylindrical grains with central perforation. More complex functions were obtained for Baria motors with plugged-in mandrels casting.

The required 3 ballistic parameters are identified by a computer routine minimizing the following error function over the entire quasi-steady burning process

$$Er = \frac{\sqrt{\int \left(p_{real}(t) - p_{calc}(t)\right) dt}}{\int p_{real}(t)\, dt}$$

being the subscripts "real" and "calc" related to the experimental and computed pressure traces respectively. For a given function a(w), the minimum of Er defines the best ballistic parameters of Vieille law for a specific shot. Since each propellant batch is tested at 2 or 3 different operating pressures, minimization of the average error is performed.

5.2 Application

This method has been applied to Baria motors produced with the mandrel-in-place during casting process. In the 70N series two motors have been fired with different operating pressures. The easiest a(w) function that brings about pressure traces close to the experimental ones is a symmetrical parabola whose integral is equal to the unit. Web thickness and burning time are correlated by the burning rate.

Here, web thickness is normalized by the initial grain thickness W_b

$$w(t) = \frac{\int r_b\ dt}{W_b}$$

$$K(w) = aw^2 + bw + c$$

$$w = 0 \quad K = HF$$

$$w = 1 \quad K = HF$$

$$\int_0^1 K\ dw = 1$$

Under these two conditions, the curve is completely defined if the value HF (Hump Factor) is fixed. HF = 1.0 means no correction. The best results, which means lowest error, are given by HF between 0.95 and 0.85.

Here is a comparison between experimental and calculated pressure traces from the proposed model. For the 70N series, with an imposed value of HF=1.0 one finds for the ballistic parameters

$$a = 1.944 \text{ mm} / (\text{bar}^n)$$
$$n = 0.367$$
$$Er = 4.91\%.$$

By letting HF free, the approximation is improved and for HF=0.90 one finds

$$a = 1.930 \text{ mm} / (\text{bar}^n)$$
$$n = 0.369$$
$$Er = 3.60\%.$$

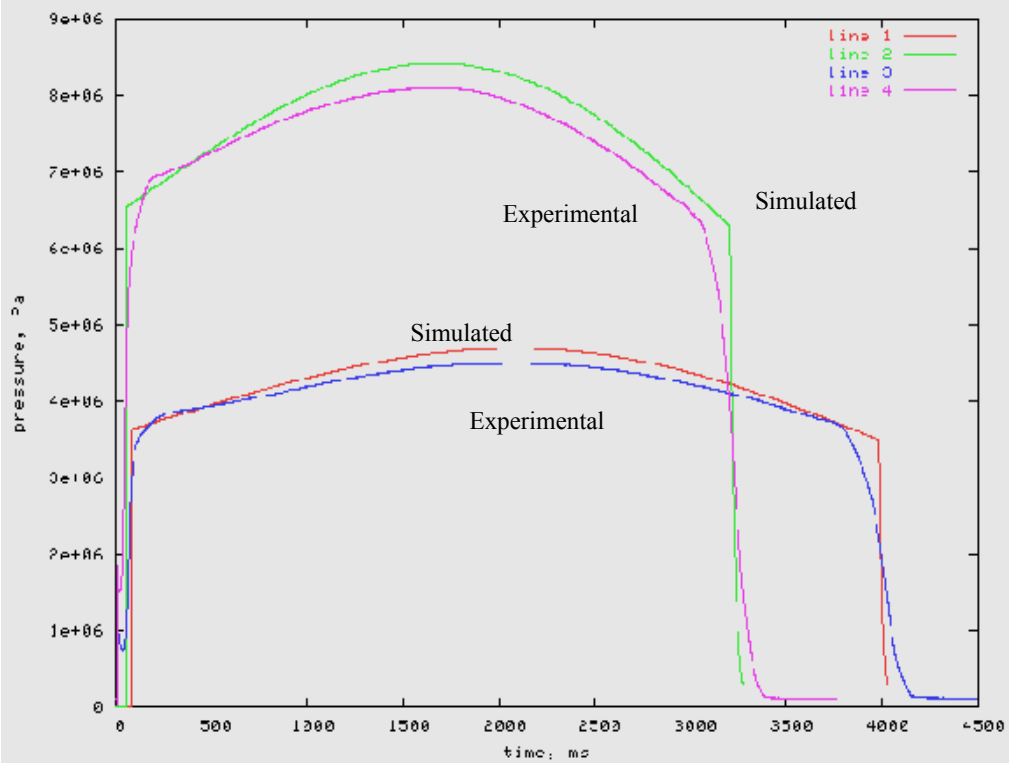

Fig. 14. Experimental vs. computed pressure traces with HF=0.90 for the 70N Baria series

For comparison, if a standard data reduction procedure is applied (for example, BPD1), lower burning times and higher burning rates are deduced.

5.3 Comments

The procedure here proposed is able to reproduce the instantaneous burning rata of the motor during its quasi-steady regime. This allows to identify the ballistic parameters taking into account the whole burning process. The proposed model is very simple. Combustion has been simulated with the addition of only one parameter (HF characterizes completely the a(w) function). Of course, transient burning effects are not accounted for and therefore the error level is magnified by this deficiency. The quasi-steady ballistic method requires more time and computing capabilities than the previous data reduction procedures, since a more sophisticated calculation is involved.

6. CONCLUSIONS AND FUTURE WORK

Data reduction from small-scale test motors can be accomplished by two different approaches, each including multiple versions. In experimental tests the actual burning rates are unknown, while errors are introduced by a variety of sources: data reduction method, specific experimental set-up (propellant, motor, instrumentation), and actual experimental running. Thus, in general, the quality of the examined methods can only be assessed based on statistical indices.

In treating simulated pressure traces, HG two-point procedure provided excellent results; but while other methods are automated, HG still requires a visual analysis of each trace. In simulated motors, HG procedure is not affected by non-idealities due to burning (nozzle erosion, non-instantaneous burnout, bore offset, etc.) and proved to be a very reliable method in terms of reproducibility and accuracy. In real motors, non-idealities restrict the accuracy demonstrated by HG in ideal cases and favor in principle the class of MB vs. TOT methods.

For real world applications to Ariane–5 boosters, improving quality and reproducibility of experimental data is more important than perfecting current data reduction methods. Indeed, test variability proved markedly larger than variability due to procedures. In particular, the industrial, time-averaged pressure, TOT methods routinely used in Europe (BC, BPD-1, BPD-2, and SNPE) produce results that are quite similar in terms of mean values and variability; improvement of these four methods should essentially concentrate on ways to evaluate the pressure integral. In addition, all tested methods – once normalized - yield the same burning rate and very similar ballistic parameters (a and n); only mean values are different. More specific trends also emerge but are dependent on the specific Baria experimental setup. For the Baria S1 setup, PM and PM-n (or POLIMI and POLIMI-n) produce, relative to TOT methods, lower exponents and lower rates, while HG produces lower exponents and higher rates. PW yields the same low exponent as other MB procedures, whereas rates depend on the enforced IR value (rate decreases for increasing IR); a value of IR $\approx$ 0.99 seems suitable for S1 at reference pressure. Different trends, however, are observed for the Baria S2 and S3 setups. In this respect, the flexibility of PW is handy in order to match a given rate (measured or not).

Analysis of burning surface evolution during combustion helps both to understand if motors behave as ideally expected and to single out anomalies within a test series. Different trends are observed for motors loaded with plunged mandrel and cast-in-place mandrel grains. The experimental pressure traces obtained with the cast-in-place mandrel motors are easily reproduced by a quasi-steady technique assuming a Vieille law with a rate factor a(w) parabolically depending on instantaneous web thickness.

Running automatic procedures on a standard laptop, times to analyze a full Ariane-5 booster segment (27 or 30 fire tests) are around few minutes for all automated methods. Analysis time of HG, being not yet fully automated, depends on datasets; about a working day is needed for full analysis of each segment. The quasi-steady ballistic method requires tens of minutes.

As to future work, it is believed important to further widen the whole experimental databank with pressure traces acquired by different grain processing techniques and different manufacturers. A relevant benefit will be gained by improving the experimental setup and test conduction of small-scale fire runs to reduce test variability. The instantaneous quasi-steady ballistic method will further be investigated to allow for transient effects and extended to plunged mandrel grains.

ACKNOWLEDGMENTS

The financial support of ASI Contract No. I/R/187/01 for this investigation is gratefully acknowledged.

REFERENCES

[1] Fry R.S. et al., *Evaluation of Methods for Solid Propellant Burning Rate Measurements*, RTO-TR-043, February 2002.

[2] Fry R.S. et al., *Solid Propellant Burning Rate Measurement Methods Used Within the NATO Propulsion Community*, 37th AIAA Joint Propulsion Conference and Exhibit, 8-11 Jul 01, AIAA Paper No. 2001-3948.

[3] Fry R.S. et al., *Evaluation of Methods for Solid Propellant Burning Rate Measurements*, presented at the Specialists' Meeting on "Advances in Rocket Performance Life and Disposal for Improved System Performance and Reduced Costs", RTO/AVT-088, Aalborg, Denmark, 23-26 Sep 2002, paper 34.

[4] Servieri M., *Sensibilità Termica e Velocità di Combustione Stazionaria di Propellenti Solidi Compositi*, M.Sc. Thesis in Aerospace Engineering, Dipartimento di Energetica, Politecnico di Milano, Milan, Italy, Feb 99.

[5] Pace F., *Internal Ballistics of Solid Propellant Small-Scale Motors*, M.Sc. Thesis in Aerospace Engineering, Dipartimento di Energetica, Politecnico di Milano, Milan, Italy, Feb 00.

[6] Morandi C., *Applicazione del Metodo HG alla Riduzione Dati Balistici*, M.Sc. Thesis in Aerospace Engineering, Dipartimento di Energetica, Politecnico di Milano, Milan, Italy, Oct 01.

[7] DeNigris A., *Metodi di Riduzione Dati Balistici da Motori a Razzo in Scala Ridotta*, M.Sc. Thesis in Aerospace Engineering, Dipartimento di Energetica, Politecnico di Milano, Milan, Italy, Feb 00.

[8] Ratti A., *Metodi di Riduzione Dati Balistici per i Boosters a Propellente Solido di Ariane-4 e di Ariane-5*, M.Sc. Thesis in Aerospace Engineering, Dipartimento di Energetica, Politecnico di Milano, Milan, Italy, Apr 00.

[9] Maggi F., *Riduzione Dati e Analisi Balistica del Motore Baria*, M.Sc. Thesis in Aerospace Engineering, Dipartimento di Energetica, Politecnico di Milano, Milan, Italy, Apr 02.

[10] DeLuca L.T., A. DeNigris, C. Morandi, F. Pace, A. Ratti, M. Servieri, A. Annovazzi, E. Tosti, R.O. Hessler, and R.L. Glick, *Burning Rate Data Reduction of Small Scale Test Motors,* presented at 5th-ISICP, Paper 045-6-OP-CM, Stresa, Italy, 18-22 Jun 00. Proceedings edited by K.K. Kuo and L.T. DeLuca, Begell-House, New York, USA, Dec 01, pp. 146-160.

[11] DeLuca L.T., C. Morandi, A. Ratti, A. Annovazzi, E. Tosti, R.O. Hessler, and R.L. Glick, *Burning Rate Data Reduction of Ariane Boosters Small-Scale Test Motors*, 2nd European Conference on Launcher Technology "Space Solid Propulsion", Rome, Italy, 21-24 Nov 00. Published by CNES, Aug 01.

[12] DeLuca L.T., A. Ratti, A. Annovazzi, P. Iannucci, E. Porcù, R.O. Hessler, and R.L. Glick, V*ariability of Burning Rate Data from Small-Scale Test Motors*, XVI Congresso Nazionale AIDAA, Palermo, Italy, 24-28 Sep 01. Published by AIDAA, Sep 01.

[13] DeLuca L.T., A. Ratti, A. Annovazzi, P. Iannucci, E. Porcù, R.O. Hessler, and R.L. Glick, *Critical Survey of Burning Rate Measurements From Small-Scale Test Motors*, 1st International HEMSI Wokshop, "Advances in Solid Propellant Technology", 12-13 Nov 02, Birla Institute of Technology, Mesra, Ranchi, India, Tata McGraw-Hill Publishing Company Ltd, New Delhi, ISBN 0-07-047407-0, 2002, pp. 29-60.

[14] DeLuca L.T., F. Maggi, A. Annovazzi, R.O. Hessler, and R.L. Glick, *Comparative Automated Burning Rate Measurement in Ariane Solid Boosters Small-Scale Tests*, "Progress in Astronautics", Polish Astronautical Society, PL ISSN 0373-5982, Tom 27 Nr. 1, 2001, pp. 6-20.

[15] DeLuca L.T., F. Maggi, A. Annovazzi, R.O. Hessler, and R.L. Glick, *Burning Rate Reduction Methods from Small-Scale Test Motors*, presented at the Specialists' Meeting on "Advances in Rocket Performance Life and Disposal for Improved System Performance and Reduced Costs", RTO/AVT-088, Aalborg, Denmark, 23-26 Sep 2002, paper 35.

[16] Annovazzi A., DeLuca L.T., F. Maggi, R.O. Hessler, and R.L. Glick, *Progress in Automated Burning Rate Reduction Methods from Small-Scale Test Motors*, presented at ICOC-02, Presidium of the Russian Academy of Sciences, Moscow, Russia, 12-16 Nov 02. Proceedings, in press.

[17] Miller W.H. and Barrington D.K., *A Review of Contemporary Solid Rocket Motor Performance Prediction Techniques*, Journal of Spacecraft and Rockets, 7 (3) : 225-237, 1970.

[18] Hessler R.O. and Glick R.L., *Comparison of Burning Rate Calculation Methods*, JANNAF Combustion Meeting, West Palm Beach, FL, USA, 27-31 October 1997.

[19] Hessler R.O. and Glick R.L., *Behavior of Pressure Derivatives During Burnout of Simulated Rocket Motors*, JANNAF Combustion Meeting, West Palm Beach, FL, USA, 27-31 October 1997.

[20] Hessler R.O. and Glick R.L., *Error Analysis of Burning Rate Measurement Procedures*, Memorandum prepared in support of the NATO RTO/AVT WG016 and presented at the Workshop on "Errors and Noise in Energetic Material Combustion Experiments", Politecnico di Milano, Milan Italy, 15-16 March 1999.

[21] Whitney C.K., Owens T.F., Paskind J., and Rubin M.B., *Scout Motor Performance and Prediction Study (PAPS)*, NASA-CR-336, NASA Langley Research Center, December 1965.

[22] Brooks W.T., *A Method for More Reproducible Burning Rate Determination*, Journal of Spacecraft and Rockets, Vol. 7, No. 12, December 1970.

[23] Brooks, W.T., "Workshop Report: Burn Rate Determination Methodology," CPIA Publication 347, Vol. II, October 1981, pp. 183-191.

[24] Timnat Y.M., *Advanced Chemical Rocket Propulsion.* Academic Press, London, UK, 1987, p. 85.

[25] Hessler R.O. and Glick R.L., *Consistent Definitions for Burning Rate Measurement in Solid Rocket Motors*, FGV Fizika Goreniya i Vzryva, Special Issue, Vol. 36, No. 1, Jan-Feb 2000. Presented at the Workshop on "Measurement of Thermophysical and Ballistic Properties of Energetic Materials", Politecnico di Milano, Milan, Italy, 22-24 June 1998.

[26] Brock F.H., *Average Burn Rate, Average Pressure Relationships in Solid Rockets*, Journal of Spacecraft and Rockets, Vol. 3, Dec. 1966, pp. 1802-1803.

[27] Glick R.L., *Reduction of Solid Rocket Data when Pressure-Time History is Non-Neutral*, Journal of Spacecraft and Rockets, Vol. 12, No. 6, June 1975, pp. 383-384.

[28] DeAmicis R., *Burning Rate Measurement at FiatAvio - Comprensorio BPD*, Private Communication, 10 October 1997. See also: Annovazzi A., *Revised Burning Rate Measurement at FiatAvio - Comprensorio BPD*, Internal Document, 1999.

[29] Ribéreau D., *Burning Rate Measurements at SNPE*, Private Communication, 29 Mar 00.

[30] Hessler R.O., Glick R.L., Tion C., Stramezzi F., and DeLuca L.T., *Characterization of Rocket Motor Acoustic Behavior*, International Workshop on Rocket Propulsion: Present and Future, Pozzuoli, Naples, Italy, 16-20 June 2002

[31] LeBreton P. and Ribéreau D., *Casting Process Impact on Small-Scale Solid Rocket Motor Ballistic Performance*, Journal of Propulsion and Power, Vol. 18, No. 6, pp. 1211-1217, 2002.

[32] Kallmeyer T.E. and Sayer L.H., "Differences between actual and predicted pressure-time histories of solid rocket motors", Paper AIAA-82-1094, 1982.